



Resources of groundwater, harmonized at
Cross-Border and Pan-European Scale

Deliverable 6.5

Water balance terms for the EU fresh groundwater grid

Authors and affiliation:
Eva Schoonderwoerd
Gualbert Oude Essink
Liduin Bos-Burgering
Deltares, The Netherlands

Tano Kivits
Willem Jan Zaadnoordijk
Hans Peter Broers
TNO Geological Survey of the Netherlands

E-mail of lead author:
Eva.Schoonderwoerd@deltares.nl

Version: final

This report is part of a project that has received funding by the European Union's Horizon 2020 research and innovation programme under grant agreement number 731166.



Deliverable Data		
Deliverable number	D6.5	
Dissemination level	Public	
Deliverable name	Water balance terms for the EU fresh groundwater grid	
Work package	WP6, Pan-EU Groundwater Resource Map	
Lead WP	TNO	
Lead Task	Deltares	
Deliverable status		
Submitted (Author(s))	21/10/2021	Eva Schoonderwoerd
Verified (WP leader)	26/10/2021	Tano Kivits
Approved (Coordinator)	26/10/2021	Hans Peter Broers



TABLE OF CONTENTS

1	INTRODUCTION	3
2	METHODOLOGY	5
2.1	Derivation of pan-European groundwater volumes.....	5
2.2	PCR-GLOBWB model description.....	8
2.2.1	Model input	9
2.2.2	Model postprocessing	9
2.3	PCR-GLOBWB model results.....	9
2.3.1	Groundwater in- and outflows	9
2.3.2	Comparison groundwater recharge map	13
3	GROUNDWATER BALANCE IN PERSPECTIVE OF GROUNDWATER VOLUMES	14
3.1	Base maps.....	14
3.2	Combination maps.....	17
4	INTERPRETATION AND DISCUSSION.....	20
4.1	Sustainable water use.....	20
4.1.1	Comparison to other studies	22
4.1.2	Consequences of groundwater overexploitation	23
4.2	Turnover time.....	24
5	CONCLUSIONS AND RECOMMENDATIONS	27
6	REFERENCES	30



1 INTRODUCTION

RESOURCE is one of the projects under the groundwater theme of the GeoERA programme of the European geological surveys (<https://www.geoera.eu>). RESOURCE is concerned with cross border aspects of groundwater. Work Package 6 provides insight in the quantity of groundwater resources at a European scale. The participating surveys have collected data about the average depths and thicknesses of the aquifers and aquitards, and the depth of the fresh-salt interface (see RESOURCE deliverable 6.2, Kivits et al., 2020). The delivered data has been aggregated to obtain EU scale information on depths and volumes of fresh groundwater (see RESOURCE deliverable 6.3, Kivits et al., 2021), thus identifying the principal fresh groundwater systems of Europe. The compiled information also yields an estimate of the total volume of fresh groundwater. The pan-European groundwater resources maps cover the countries of the participating geological surveys. To get a full coverage of Europe, we also used the global hydrological model PCR-GLOBWB (Sutanudjaja et al., 2018).

Knowledge of the fresh groundwater volume is useful for estimating the buffer capacity of the groundwater resource for (temporary) abstractions of groundwater. The volume can be an indicator of the risk to groundwater salinization of abstraction wells, the risks for droughts and the risks for land subsidence, and has a direct relation with the turnover times of the groundwater systems (e.g. Raats, 1981; Van Ommen, 1985; Haitjema, 1995).

It is important to note that the fresh groundwater volume is not directly related to the available amounts of fresh groundwater for domestic, agricultural and industrial use. The sustainability of groundwater use depends foremost on whether the water balance is closed. Therefore, this report places the volumes of fresh groundwater in Europe in the context of the main terms of the water balance: groundwater recharge and groundwater abstraction.

Similar studies have been carried out for other regions in the world of different scales (global, continental, national and regional). On a global scale, Gleeson et al. (2016) calculated volumes of groundwater that is less than 50 years old, using tritium measurements and numerical models. This young groundwater is an important resource, because it is more renewed than old ('fossil') groundwater. Also, it is more vulnerable for contamination due to the active interaction with the climate and the hydrological cycle. Gleeson et al. (2016) estimated that only a small percentage of the total volume of groundwater in the upper 2 km of the crust (22.6 million km³) is less than 50 years old (0.1-5.0 million km³). This can be compared to the global offshore fresh groundwater volume (Post et al., 2013). Zamrsky et al. (2021) and Micallef et al. (2021) estimated this total volume to be in the order of 1 million km³, based on thousands of 2D-profile models of unconsolidated porous media and over 300 aquifer databases, respectively.

On a continental scale, MacDonald et al. (2012) estimated the total groundwater storage in Africa, for which they combined the available hydrogeological and geological maps, data and literature. They also showed that for many countries it is possible to implement small-scale abstractions that are robust despite variations in recharge, but that the potential for larger-scale abstractions is much more limited. However, the access to (ground)water can improve economic growth and help to move people out of poverty. In this context, groundwater is a more reliable water source than surface water, since it is less influenced by climate meteorological variabilities



like droughts (Malakoff et al., 2020). This stresses the need for good estimations of the sustainability of groundwater abstractions, without depleting the available resources.

In addition, an estimation of groundwater volumes on a national scale can be found in Thorweihe et al. (2002), who assessed the groundwater resources in the Nubian Aquifer System, which largely spans Egypt and parts of Sudan, Libya and Chad. They showed that the groundwater in this aquifer was formed in the Late Pleistocene (over 20.000 years ago) or during the Holocene (between 14.000 and 4000 years ago). Since the current groundwater recharge is very limited, the extraction of the water of this aquifer will be non-renewable.

This shows again that the sustainability of groundwater resources is not directly related to the amount of fresh groundwater even if the volume is large compared to for instance the annual abstraction domestic, agricultural and industrial uses. This is illustrated by two examples.

First, the Mekong Delta contains approximately 867 km³ fresh groundwater (Gunnink et al., 2021), while about 1 km³ groundwater was extracted in 2017 (Minderhoud et al., 2017). Yet, the Mekong delta experiences groundwater level drawdowns up to more than 20 m (Erban et al., 2014) and land subsidence of on average ~18 cm over the past 25 years, as a consequence of groundwater abstraction (Minderhoud et al., 2017; Neussner, 2019). Pham et al. (2019) demonstrate that most fresh groundwater infiltrated the subsurface during a period of low sea-level, at least more than 20.000 years ago. Sedimentation during the last 20.000 years has increased the resistance of the top layer and this currently prevents fresh groundwater from recharging the deeper aquifers.

Second, for the Netherlands, the fresh groundwater volume is estimated to be ~1100 km³ (Stuurman et al., 2008) while the total groundwater abstraction is only ~1.5 km³ per year. Still, in 1989 more than 20% of the abstraction wells has been abandoned due to salinisation (Stuyfzand, 1993) and low groundwater levels during dry years have serious impact on nature, buildings, infrastructure and agriculture (Witte et al, 2020).

With these notions at hand, this report places the volumes of fresh groundwater in Europe in the context of the main terms of the water balance: groundwater recharge and groundwater abstraction. The results of the analysis are subsequently discussed and interpreted in terms of sustainable water use and turnover times. The report should be considered as a first approach and estimate of the water balance terms, and recommendations are given for future research on this theme.



2 METHODOLOGY

2.1 Derivation of pan-European groundwater volumes

One of the main objectives of the RESOURCE WP6 project was to come to a first estimate of the groundwater volumes in the participating countries. Using the information that the surveys gathered in the template (see RESOURCE D6.2, Kivits et al., 2020), the first maps were presented in deliverable 6.3 (Kivits et al., 2021). Here, we present a short overview of the used method as well as the latest versions of the groundwater volume map.

The map of the total groundwater volume (see Figure 2.1) was made based on information that the RESOURCE WP6 participants gathered in the template using an existing 10 km X 10 km INSPIRE grid which covers Europe. Each survey defined a number of groundwater layers within each grid cell in their country. For each of those layers, information was gathered on thickness, extent, ages, hydrogeofacies, hydrological parameters etc. was gathered. Since the goal of this project was to define fresh groundwater volumes and depths, layers were defined up to a depth that is relevant for the available flowing fresh groundwater. Depending on the groundwater system, the bottom depth was defined in different way:

- by a fresh-salt interface (described by either a chloride concentration of 1000 mg/l Cl⁻, an amount of total dissolved solids of 1500 mg/l TDS or an electrical conductivity of 2500 μ S/cm)
- by a hydrogeological boundary that prevents further downward flow. This could for example be a thick clay layer with high resistance or the vertical extent of the fractured zone in karst systems.

For more information on the parameters that were used and how they are defined we refer to deliverable 6.2 (Kivits et al., 2020).

The total groundwater volume as shown in the maps are calculated using a number of parameters in the template. First, a selection is made for the saturated layers, to exclude the unsaturated zone from the calculations on total groundwater volumes. Second, a selection is made for the aquifers, to exclude the volume of groundwater in aquitards for the calculation of total volume. Third, the thickness of each saturated aquifer with fresh groundwater is multiplied by the extent of that layer (the percentage that the layer covers the 10 km X 10 km grid cell) and the porosity to reach the volume of groundwater in that layer. Fourth, all layer volumes are then added together to reach the total groundwater volume.

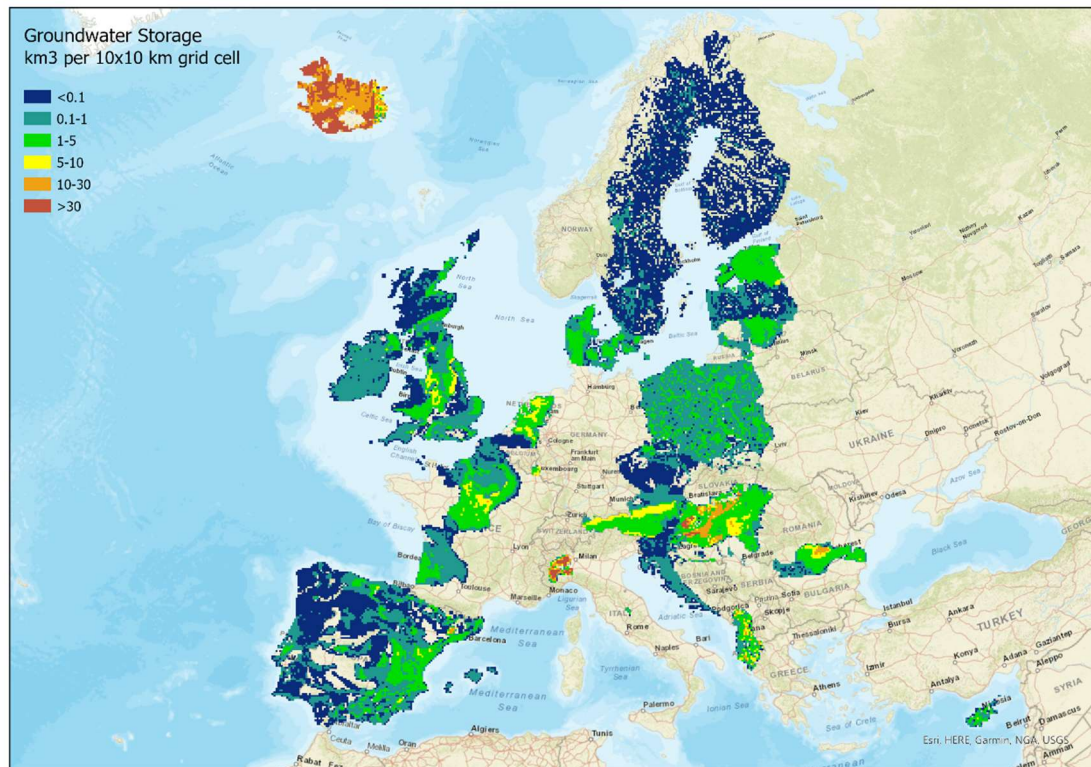


Figure 2.1 Map showing the total fresh groundwater volume over Europe in km^3 per 10 km x 10 km grid cell.

Figure 2.1 shows the map of the total fresh groundwater volume in aquifers in km^3 per 10x10 km grid cell for the participating countries of RESOURCE WP6. The map reveals the wide range of groundwater volumes in aquifers over Europe. The values range from less than 0.1 to approximately 50 km^3 per 10 km X 10 km grid cell, with generally high volumes in sedimentary basins and sometimes in karstified areas. The map gives an overview from the southwest of Portugal and Spain to the very northeast of Finland, and from the southeast of Cyprus to the northwest of Iceland, covering a large part of Europe. Unfortunately, there are blank areas on the map, which is either due to geological surveys of countries/regions not participating in WP6 or a lack of data or available time within this project to fill the grid for the entire management area.

We have also created a map of groundwater volume in the upper 100 m to better represent the volume of water that can be used economically (see Figure 2.2). This map is used along the map of the total fresh groundwater volume for the calculations of the water balance as presented in Chapter 3. This volume is calculated by adding volumes together from the saturated aquifers until the cumulative layer thickness (including aquitards) reaches 100 m.

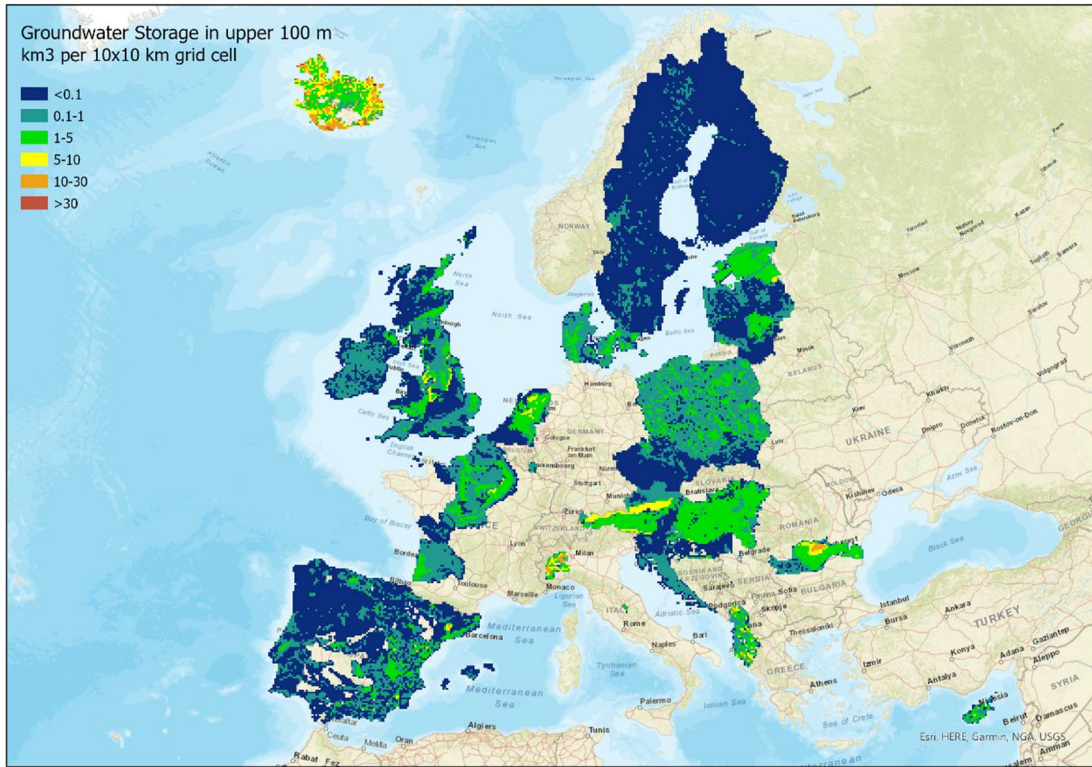


Figure 2.2 Map showing the total groundwater volume over Europe in the upper 100 m in km³ per 10 km X 10 km grid cell.

2.2 PCR-GLOBWB model description

The PCR-GLOBWB model (Sutanudjaja et al., 2018) is used to derive an estimate of the EU water balance. It is a 5 arcmin (approximately 10 km X 10 km) global hydrological and water resources model, developed in Python and PC Raster by Utrecht University in the Netherlands. The model is able to calculate sector-specific water demand, ground- and surface water abstraction, water consumption and return flows. Figure 2.3 shows a conceptual overview of a PCR-GLOBWB cell and the states and fluxes that are modelled. For a more extensive description of the PCR-GLOBWB model, we refer to Sutanudjaja et al. (2018).

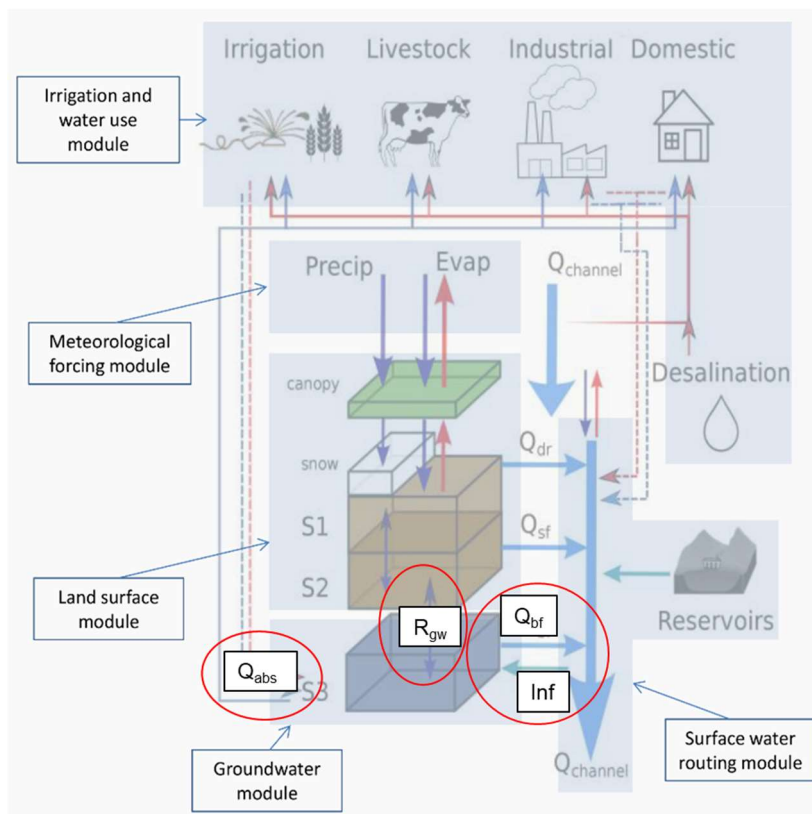


Figure 2.3 Conceptual overview of a PCR-GLOBWB model cell with the various states and fluxes (Figure adapted from Sutanudjaja et al., 2018).

The PCR-GLOBWB model runs, including the pre- and postprocessing, have been carried out in the Delft-FEWS computation framework (Werner et al., 2013; also see <https://oss.deltares.nl/web/delft-fews>). This system is an open data handling platform that contains a collection of modules designed for building a hydrological forecasting system and is able to connect many different models.

We selected the PCR-GLWWB fluxes that are part of the groundwater balance. As shown in Figure 2.3, there are four relevant fluxes:

- Groundwater recharge (R_{gw});
- Groundwater abstraction (Q_{abs});
- Riverbed infiltration (Inf);
- Baseflow to the surface water (Q_{bf}).

The groundwater recharge (R_{gw}) contains all water flows that percolate from the soil into the groundwater. Riverbed infiltration (Inf) can only occur when the groundwater discharge to the



surface water (Q_{bf}) is zero due to a groundwater level lower than the surface water level. The amount of abstracted groundwater (Q_{abs}) is calculated every timestep (of 1 day) by first estimating the water demands for irrigation, livestock, industry and households. The demand is translated to an actual water withdrawal based on the water availability. Water can be withdrawn from both surface water and groundwater; based on the fractions of the available surface- and groundwater it is determined from which source the water will be abstracted. Water can be sourced from cells nearby the location with water demand, but since there is no global data available on water redistribution networks, the water availability is pooled over zones of ~ 1 arcdeg by 1 arcdeg (for surface water) and ~ 0.5 arcdeg by 0.5 arcdeg (for groundwater). There are return flows associated with the withdrawn water. For irrigation, the water that is not lost by transpiration or evaporation will percolate to the groundwater as groundwater recharge. The water withdrawn for the other sectors is partly flowing back to the surface water as a return flow, based on a country-specific recycling ratio.

2.2.1 Model input

The meteorological forcing of the model is the ERA5 data set (Copernicus Climate Change Service, 2017). The parameters have a temporal resolution of 1 day, except for the input of the years 2019 and 2020, which have hourly data. This data is aggregated to a daily timestep. The meteorological parameters from the ERA5 data set that are used, are:

- Total precipitation (TP)
- Radiation shortwave down (SSRD)
- 2 meter temperature (2T)
- Mean sea level pressure (MSL)
- Extraterrestrial solar radiation down (TSRD)

The PCR-GLOBWB submodels that are selected to be able to simulate the whole of Europe are the submodels 3, 26, 27, 32 and 33. The model is run for the simulation period 2000-2020, the results of the period 2010-2020 will be used in the further analysis. Following this procedure, there is a 10-year period of model spin-up time.

2.2.2 Model postprocessing

The PCR-GLOBWB results are aggregated to monthly output maps at 5 arcmin X 5 arcmin resolution. This output is regridded to a 10 km X 10 km spatial grid, to be able to further process and compare the results with other output of GeoERA RESOURCE. An area weighted average within the gridcells of the 10 km X 10 km destination grid is used to determine the output for this grid. This means that some local maxima and minima will be reduced.

2.3 PCR-GLOBWB model results

2.3.1 Groundwater in- and outflows

As discussed in section 2.2, there are four fluxes that comprise the groundwater in- and outflow. The maps of these fluxes are shown in this section. The maps show the long-term average flux (in the unit mm/year) of the whole model period (2010-2020).

The main water inflow is the groundwater recharge R_{gw} (Figure 2.4), which in PCR-GLOBWB is the flux of all water that percolates down from the soil to the groundwater table. Note that this not the same as the effective precipitation, being the difference between the precipitation and



actual evaporation. The effective precipitation is further partitioned into groundwater recharge (R_{gw}), surface flow (Q_{dr}) and interflow (Q_{inf}), see Figure 2.3. Most groundwater leaves the groundwater volume as groundwater discharge Q_{bf} (baseflow) (Figure 2.5). As discussed in section 2.2, riverbed infiltration (Inf) (Figure 2.6), which is negative groundwater discharge, only occurs at locations of a river and where the groundwater discharge (Q_{bf}) becomes zero. Figure 2.7 shows the groundwater abstraction (Q_{abs}). Note that the groundwater abstractions are pooled within a region of 30 arcmin X 30 arcmin (6 X 6 model cells), which causes the larger spots in Figure 2.7 in which the abstractions are high.

Figure 2.7 shows that the calculated groundwater abstractions are high in regions with a high population density. The groundwater abstraction is calculated based on the water demand of different sectors (irrigation, livestock, industry, households). The land use and population density will therefore influence the locations with high water demand and water withdrawal.

Recharge (mm/year). PCR-GLOBWB output. Average 2010-2020

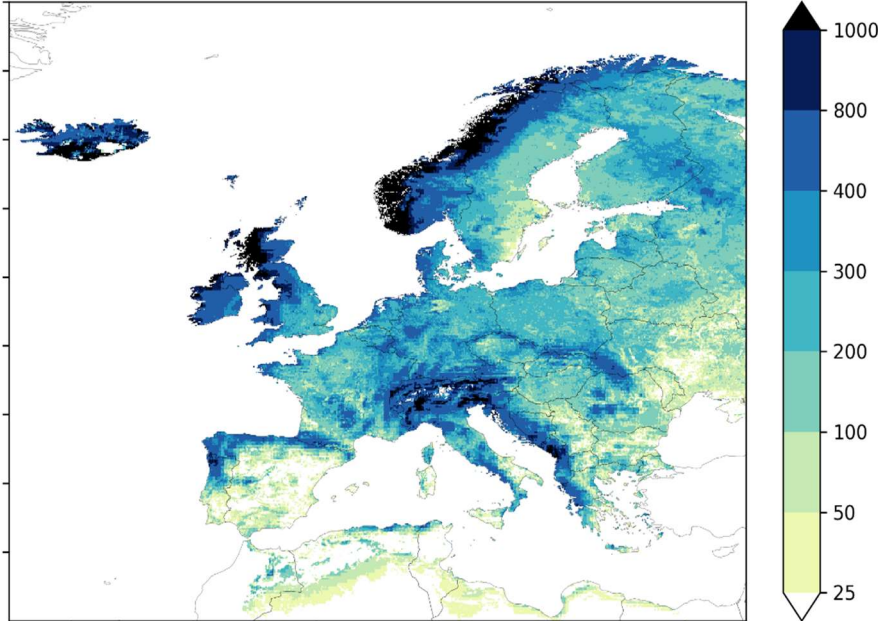


Figure 2.4 Average groundwater recharge (R_{gw}) (mm/year) according to the PCR-GLOBWB model (average over 2010-2020). Note that the difference with Figure 2.5 is small: most recharge leaves the groundwater system to the surface water system.

Average groundwater discharge to surface water (mm/year).
Average 2010-2020

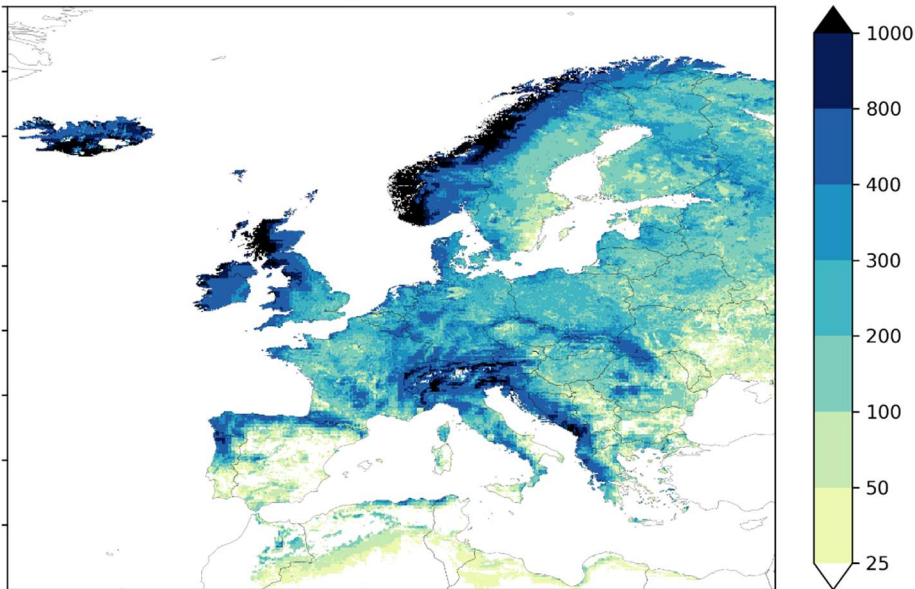


Figure 2.5 Average groundwater discharge (Q_{bf}) to surface water (mm/year) according to the PCR-GLOBWB model (average over 2010-2020). Note that the difference with Figure 2.4 is small: most recharge is discharged to the surface water system.

Average surface water infiltration (mm/year). Average 2010-2020



Figure 2.6 Average surface water infiltration (I_{nf}) (mm/year) according to the PCR-GLOBWB model (average over 2010-2020).

Average groundwater abstraction (mm/year)

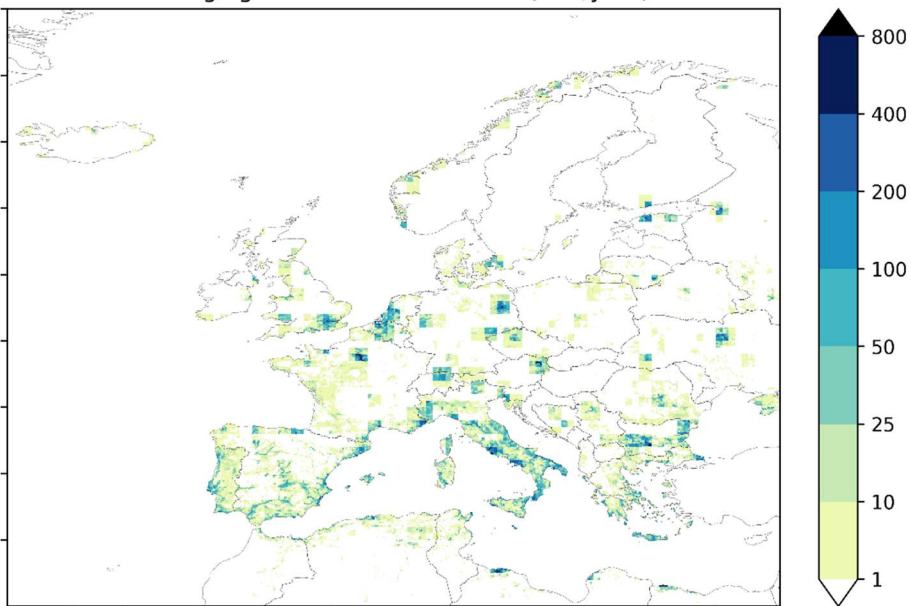


Figure 2.7 Average groundwater abstraction (Q_{abs}) (mm/year) according to the PCR-GLOBWB model (average over 2010-2020).

2.3.2 Comparison of groundwater recharge maps

A pan-European groundwater recharge map has been developed within the ‘TACTIC’ project on groundwater and climate change within the GeoERA programme (Martinsen et al., 2021). This map is shown next to the groundwater recharge output of the PCR-GLOBWB model in Figure 2.8. The groundwater recharge according to the PCR-GLOBWB model is generally higher compared to the pan-European map that was developed within TACTIC. There are several explanations that causes this discrepancy (Martinsen et al., 2021):

1. Both maps are based on different climate forcing data. The PCR-GLOBWB model uses the global ERA5 dataset, whereas the TACTIC map is developed using the European E-OBS data. For several countries (Denmark, UK, France, Spain and the Netherlands), the national precipitation dataset as supplied by the national meteorological office was used;
2. The maps show the yearly average over different periods. The PCR-GLOBWB map is a yearly average of 2010-2020, the TACTIC map is a yearly average of 1981-2010;
3. The groundwater recharge as calculated by PCR-GLOBWB consists of all fluxes that flow from the subsurface into the groundwater, including the part of the irrigation water that is not lost by transpiration and evaporation, while the TACTIC map represents only the recharge from precipitation;
4. The model concept of PCR-GLOBWB might influence the results in regions with high topographic differences, since the fluxes (the percolation and subsurface stormflow/interflow) are averaged within a model cell which may result in a underestimation of the effect of the variation of the surface level and the distance to bedrock.

These differences confirm that the actual groundwater recharge is difficult to estimate correctly (Döll and Fiedler, 2007). The map developed within TACTIC is based on more local data, so these fluxes might be closer to reality compared to the result of the global PCR-GLOBWB model. However, we have used the PCR-GLOBWB modelled groundwater recharge for the rest of this study, to be able to work with a consistent set of water balance terms.

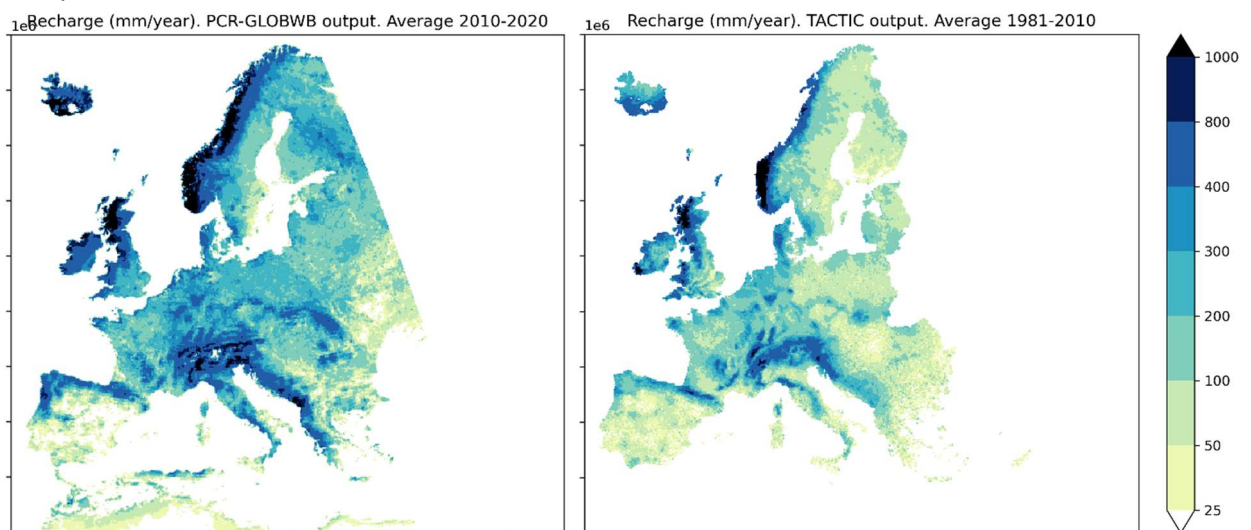


Figure 2.8 Left: average groundwater recharge (mm/year) (2010-2020) as calculated by PCR-GLOBWB. Right: average groundwater recharge (mm/year) (1981-2010) as calculated within the GeoERA TACTIC project (Martinsen et al., 2021).

3 GROUNDWATER BALANCE IN PERSPECTIVE OF GROUNDWATER VOLUMES

3.1 Base maps

Starting point for the analysis are three base maps: recharge, abstraction and volume. The maps have been prepared using the PCR-GROBWB model (recharge and abstraction) and the RESOURCE volumes grid (volume). These quantities are aggregated over the level 1 NUTS regions (Nomenclature of territorial units for statistics), which are the major socio-economic regions of Europe (see [https://ec.europa.eu/eurostat/statistics-explained/index.php?title=Glossary:Nomenclature_of_territorial_units_for_statistics_\(NUTS\)](https://ec.europa.eu/eurostat/statistics-explained/index.php?title=Glossary:Nomenclature_of_territorial_units_for_statistics_(NUTS))). It should be stressed that the regions vary in surface area, which has a major influence on the volumes per region. The base map with the aggregated groundwater abstraction is shown in Figure 3.1, the aggregated groundwater recharge in Figure 3.2, the aggregated fresh groundwater volume in Figure 3.3. The regions with a small volume or flux are mostly also regions with the smaller surface area.

The fresh groundwater volumes are not known for all regions because not all countries participated in GeoERA RESOURCE (or due to a lack of data or available time to finish the complete the country grid). Only the NUTS regions are shown where a volume is known for at least 50% of the region (Figure 3.3). In the further comparison with the groundwater recharge and abstraction, these maps are also masked for the regions where the fresh groundwater volume is known. The volume base map has also been prepared for the groundwater volumes within the upper 100 m (Figure 3.4).

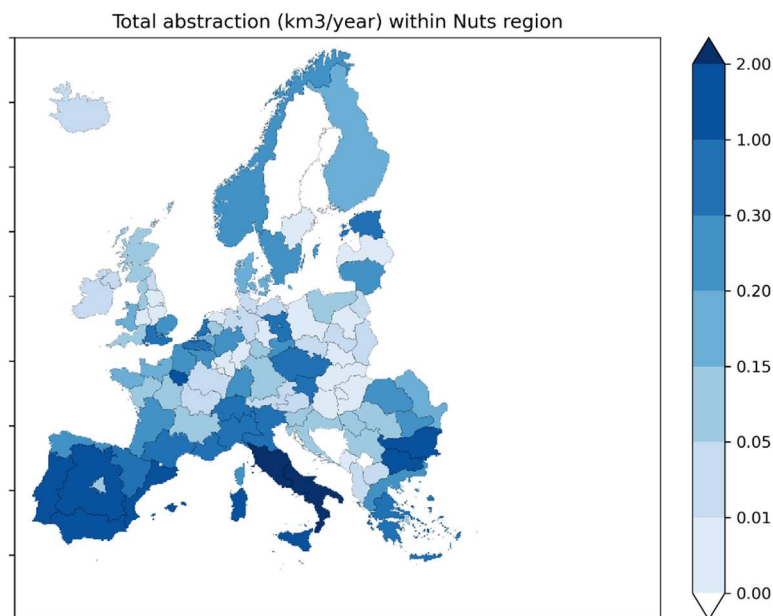


Figure 3.1 Aggregated average groundwater abstraction (km³/year) in the period 2010-2020, according to the PCR-GLOBWB model. The abstractions are summed within a NUTS 1 regions. Note that the regions have different surface areas.

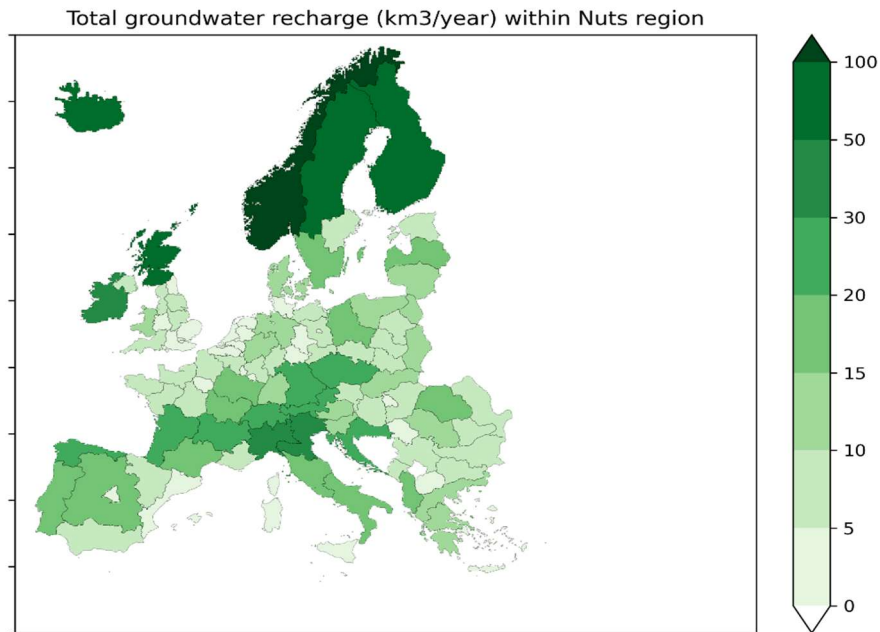


Figure 3.2 Aggregated average groundwater recharge (km³/year) in the period 2010-2020, according to the PCR-GLOBWB model. The groundwater recharge is summed within NUTS 1 regions. Note that the regions have different surface areas.

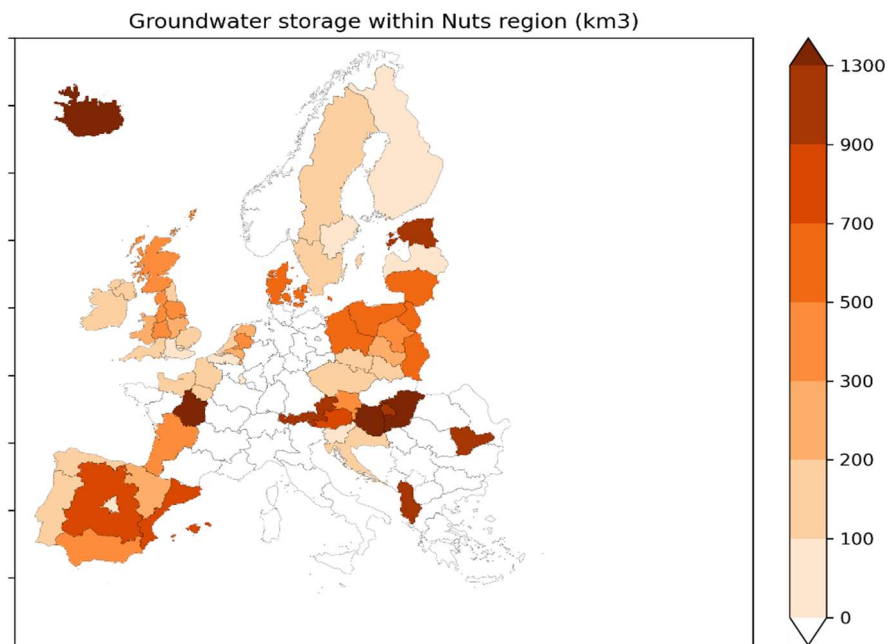


Figure 3.3 Aggregated total groundwater volume (km³). The groundwater volume is summed within NUTS 1 regions for those regions where the volume is known in at least 50% of the grid cells. Note that the regions have different surface areas.

Shallow groundwater storage within Nuts region
in the upper 100 m of the subsurface (km³)

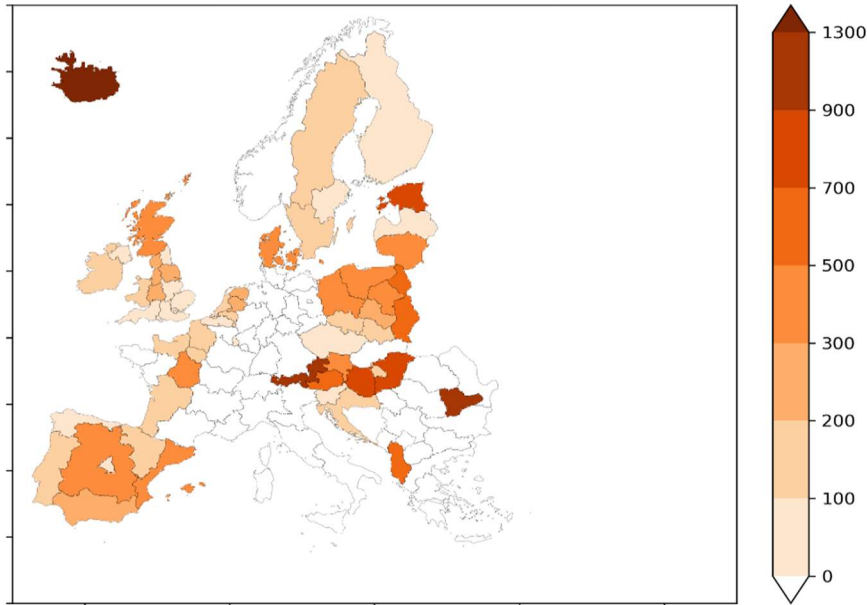


Figure 3.4 Aggregated shallow groundwater volume (km³), in the upper 100 m. The groundwater volume is summed per NUTS 1 region for those regions where the groundwater volume is known for at least 50% of the grid cells. Note that the regions have different surface areas.

3.2 Combination maps

The base maps that were shown in the previous section are combined to create three maps that give an indication of the sustainability of the groundwater abstractions and the robustness and turnover times of the groundwater system. For every combination map, there is a scheme that shows how basemaps are combined.

The first combination map shows the fraction of the groundwater recharge volumes that is extracted from the groundwater within a NUTS region. As can be seen in Figure 3.5, this combination map is made by dividing the recharge base map (Figure 3.2) by the abstraction base map (Figure 3.1).

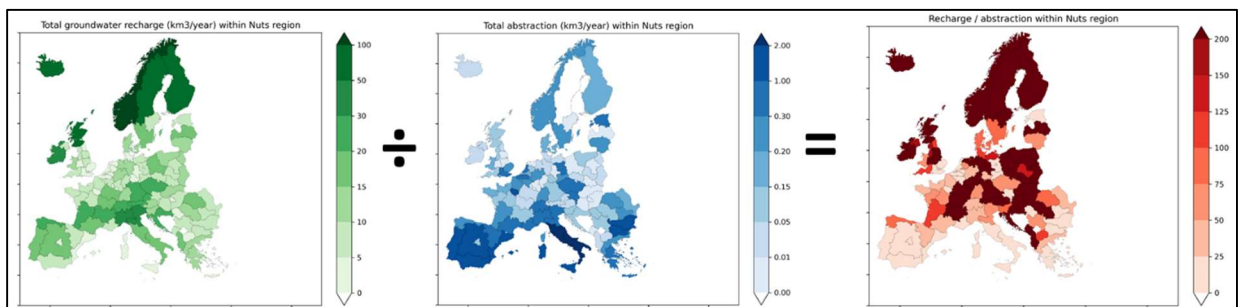


Figure 3.5 Scheme showing the calculation of the map of the groundwater recharge/abstraction shown in Figure 3.6: the aggregated groundwater recharge within a NUTS region (left figure) is divided by the aggregated groundwater abstraction within a NUTS region (middle figure), which results in the map of Figure 3.6.

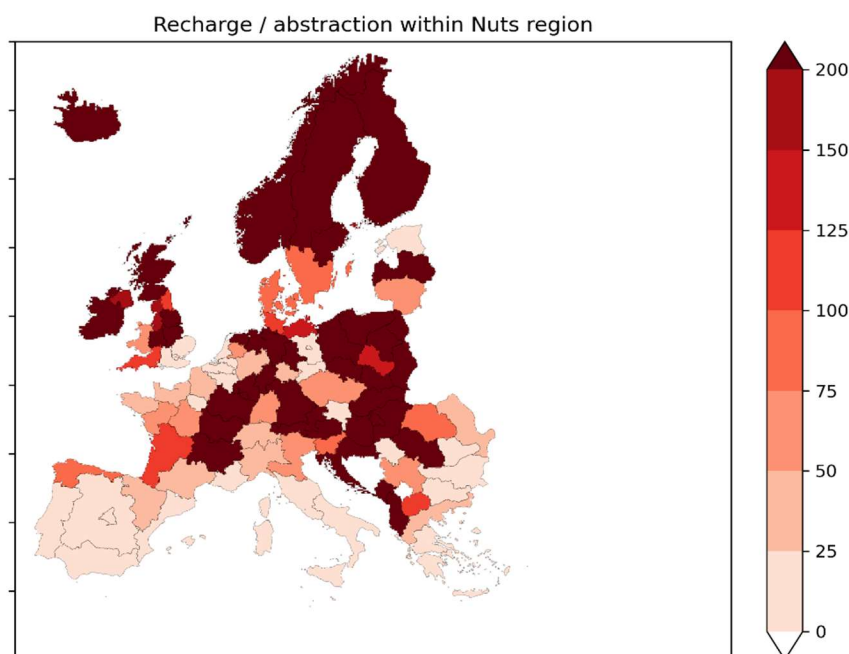


Figure 3.6. Yearly average groundwater recharge within a NUTS 1 region (km^3/year), divided by yearly average abstraction (km^3/year) within a NUTS 1 region (-). Both fluxes are calculated output of the PCR-GLOBWB model.

The second combination map shows the fraction of the total groundwater volume that is extracted from the groundwater. Figure 3.7 illustrates that it has been constructed by dividing the volume base map (Figure 3.3) by the abstraction base map (Figure 3.1). Since the groundwater volumes are not known everywhere, the groundwater extraction map is masked for the location where the groundwater volumes are known. Only the NUTS regions are shown where at least 50% of the groundwater volume is known.

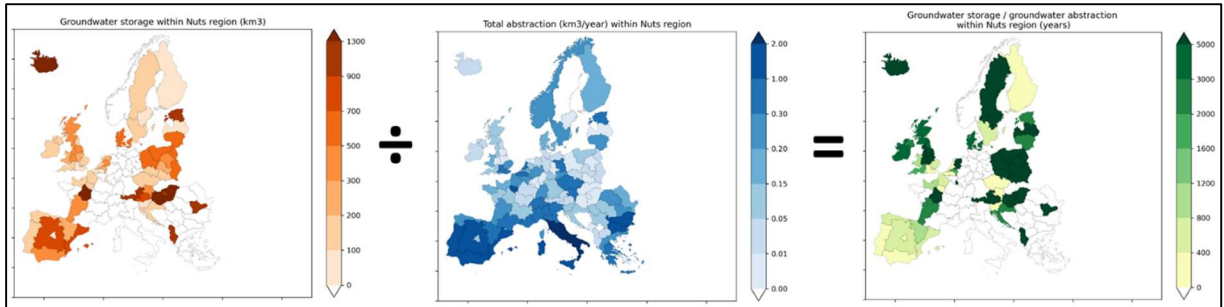


Figure 3.7 Scheme showing the calculation of the map of the volume/abstraction shown in Figure 3.8: for the locations where the groundwater volume is known, the aggregated groundwater volume within a NUTS region (left figure) is divided by the aggregated groundwater abstraction within a NUTS region (middle figure), which results in the map of Figure 3.8.

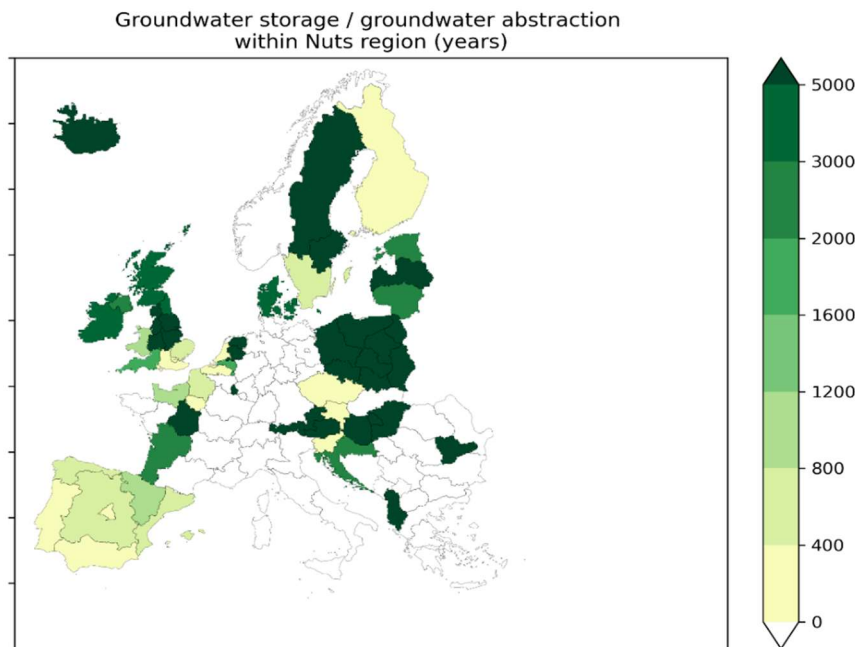


Figure 3.8 The total groundwater volume (km^3) divided by the total groundwater abstraction (km^3/year) within a NUTS region.

The third combination map shows the fraction of volume base map (Figure 3.3 or Figure 3.4) divided by the recharge base map (Figure 3.2). The derivation is shown in Figure 3.9. Similar to Figure 3.8, this combination map is masked for the locations where the groundwater volume is known.

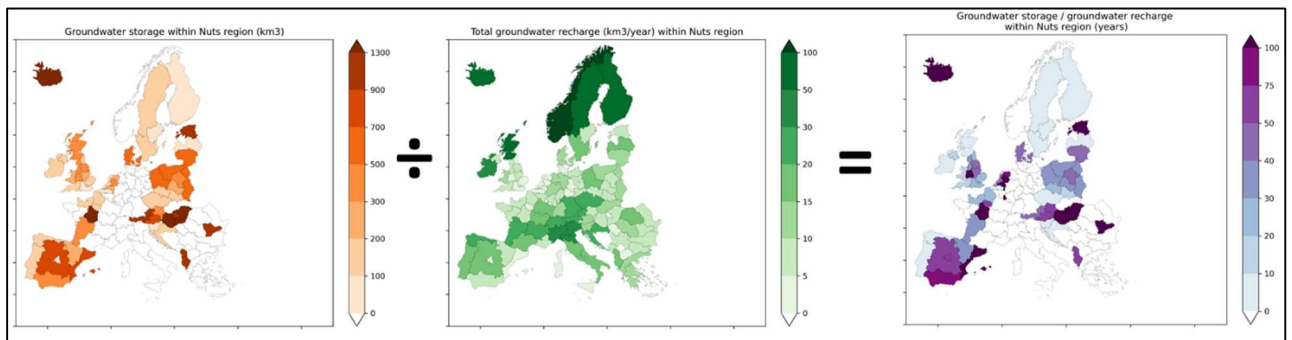


Figure 3.9 Scheme showing the calculation of the map of the volume/recharge shown in Figure 3.10: for the locations where the groundwater volume is known, the aggregated groundwater volume within a NUTS region (left figure) is divided by the aggregated groundwater recharge within a NUTS region (middle figure), which results in the map of Figure 3.10. Note that Figure 3.10 shows a combination map both for the total groundwater volume and for the shallow groundwater volume.

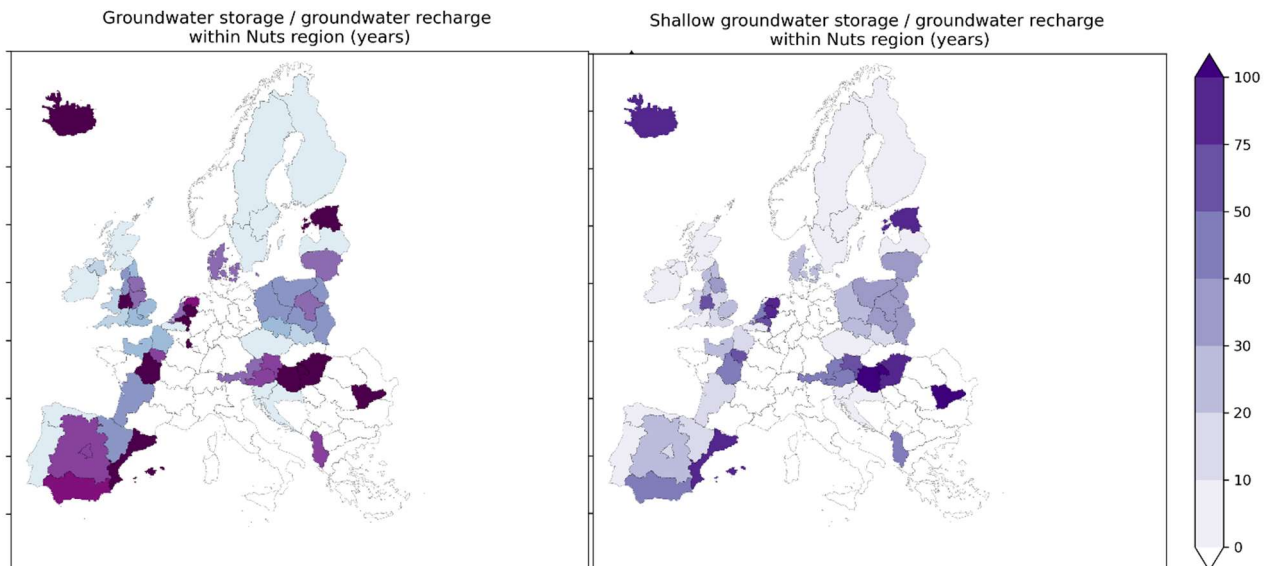


Figure 3.10 The total groundwater volume (km^3) divided by the groundwater recharge (km^3/year), which shows the turnover time of the groundwater. Left: turnover time based on the complete available groundwater volume. Right: turnover time for the volume in the upper 100 m of the subsurface.

4 INTERPRETATION AND DISCUSSION

4.1 Sustainable water use

Figure 4.1 (which is a copy of Figure 3.6, reproduced below for convenience) shows the fraction of groundwater recharge over groundwater abstraction. Groundwater recharge is the main water source of groundwater, with infiltration of river water as second best. When the recharge-abstraction ratio is high, there is much more recharge compared to the abstractions in a region, whereas a low recharge-abstraction fraction shows that the abstracted water is close to the amount of recharge. Below a value of 1, the amount of abstracted groundwater is larger than the groundwater recharge and the groundwater resources definitely is overexploited. The abstraction is not sustainable, and the resource will become depleted; the pace of depletion depends among others on the hydrogeological conditions and the total fresh groundwater volume that is available. The dark regions in the map have low groundwater abstractions relative to the groundwater recharge, in general indicating more sustainable abstractions. Within the light regions, the abstracted volumes are closer to the recharge. These regions are more susceptible to non-renewable groundwater abstraction. Even if the ratio is larger than one, the abstractions may not be sustainable, depending on e.g. environmental flow needs and the level at which the groundwater is abstraction and the amount of recharge that infiltrated into deeper aquifers.

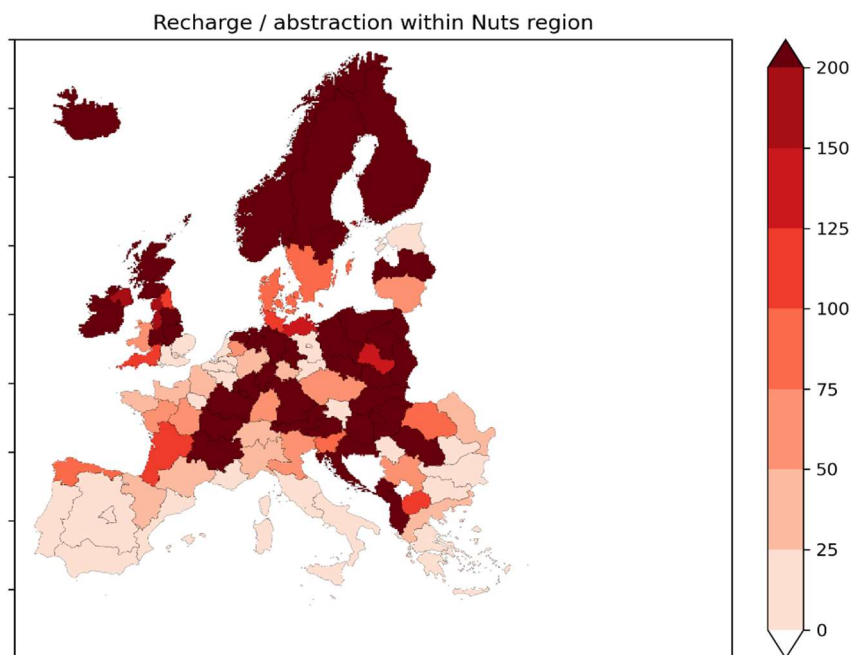


Figure 4.1. This is a copy of Figure 3.6. Yearly average groundwater recharge within a NUTS region, divided by yearly average abstraction within a NUTS region (-). Both fluxes are calculated output of the PCR-GLOBWB model.

As can be seen in Figure 4.1, the Mediterranean regions have groundwater abstractions in the class of the lowest sustainability. The groundwater recharge in these regions is limited, so even for small abstracted groundwater fluxes, the fresh groundwater volume may decline. Note that Custodio already pointed this out in 1987 and 2002 (Custodio and Bruggeman, 1987; Custodio, 2002). Other regions that are at risk are densely populated urban areas, like the South-East of

the United Kingdom, the West and South of The Netherlands, Belgium, Estonia and the regions around Berlin and Paris. Though these regions receive a significant amount of precipitation, their abstracted volumes are also large.

The combined map in Figure 3.6 (and Figure 4.1) is most representative for the long-term sustainability of the groundwater system. When abstractions are limited relative to the groundwater recharge to the system, the abstractions can be sustained infinitely, independent of the volume of the groundwater resource. However, note that when large groundwater abstractions are concentrated in a small area, this local groundwater system of the NUTS region can still be overexploited, and the local situation might not be sustainable.

The volume of the groundwater resource becomes important when we address the robustness of the resources for seasonal and multi-year variations in recharge and abstractions, because the volume is an indicator for the *capacity to buffer* periods with very limited recharge (droughts) or to periods with large abstractions (for e.g. intercepting calamities). A larger volume means a larger buffer capacity to deal with those shorter-term imbalances. The buffer capacity is conceptually approximated in the second combination map in Figure 4.2 (which is a copy of Figure 3.8) where we use the GeoERA derived groundwater volumes.

The combination map in Figure 4.2 shows the ratio of the total available groundwater volume over the groundwater abstraction, for the regions where the fresh groundwater volumes are known. A smaller value (light colors) indicates that the abstracted fluxes are large relative to the total available groundwater volume. The values should be interpreted quite differently as the values in the first combined map of recharge and abstraction (Figure 4.1). Very high values are needed for a robust system, depending on the hydrogeological settings. As mentioned earlier in the introduction, even relatively high volume-abstraction ratios can lead to serious impacts. The lowering of the groundwater heads in dry periods may cause salinization and land subsidence that is not reversible.

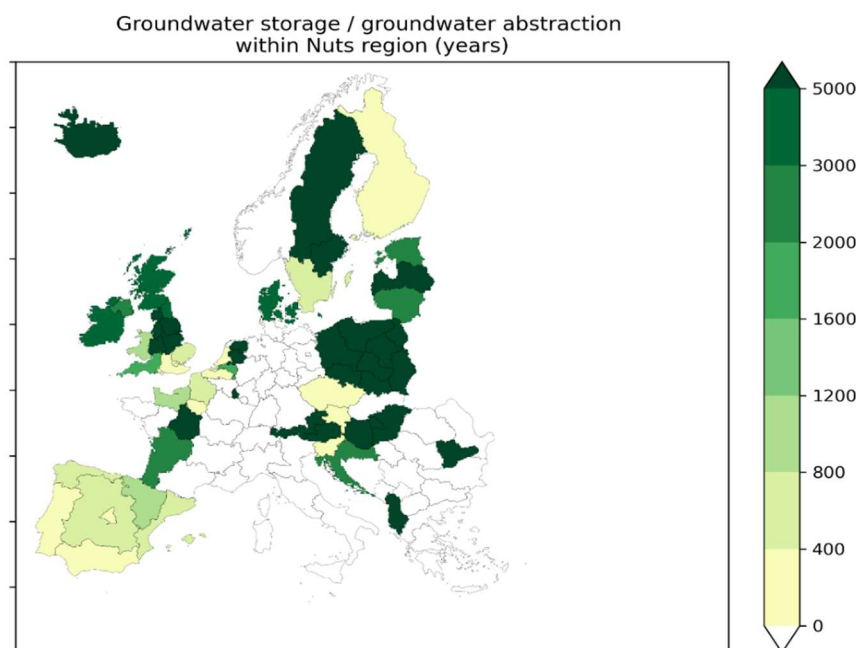


Figure 4.2 This is a copy of Figure 3.8. The total groundwater volume (km^3) divided by the total groundwater abstraction (km^3/year) within a NUTS region.



Regions with large buffer capacity (darker colors in Figure 3.8 / Figure 4.2) may also be affected by periods of drought or increased abstractions but might deal with those conditions over longer time. Conceptually, these regions are sustainable when both groundwater recharge is larger than abstraction rates (long term sustainability) and buffer capacity is large enough to overcome periods of droughts or intensive pumping (short term sustainability).

An example of vulnerable regions are the regions in Spain. According to the first combination map (Figure 3.6 / Figure 4.1), a large fraction of the yearly averaged recharge is abstracted (small recharge-abstraction fraction) while the second combination map (Figure 3.8 / Figure 4.2) shows that this extracted water is also large relative to the groundwater volume (small volume-abstraction fraction). As long as the groundwater recharge remains constant in time, the problems remain limited because the groundwater abstractions are smaller than the groundwater recharge. However, during prolonged droughts in these regions, the groundwater recharge is much lower and the abstraction higher than the average values. In this situation, the yearly extracted groundwater becomes larger than the amount that is replenished by groundwater recharge and this cannot be buffered by the system if the buffer capacity is too low (see Figure 3.8 / Figure 4.1). Together this means that the groundwater volume will rapidly decrease in periods of droughts.

In contrast, an example of a much more robust system is the Limousin region in the middle of France. The recharge-abstraction fraction in this region is relatively low, albeit still higher than the fractions found in most regions of Spain. In dry periods, the groundwater extraction might still result in a depletion of the groundwater volume, because the volume will not be replenished immediately by groundwater recharge. However, the volume-abstraction fraction is very large, which may mean that the system does not suffer irreversible changes during the dry period.

Generally, Figure 3.6 and Figure 3.8 show that there are three aspects that will influence the vulnerability of the groundwater resources in a region. First, a large total groundwater volume will result in a more robust system that can absorb fluctuations due to rapid, incidental events, like prolonged droughts, or some decennia of overexploitation. Second, a large groundwater recharge results in a system that is resilient to stresses like abstraction. Third, less groundwater abstraction causes less stress on the system. Having said this, on a local scale e.g. in a NUTS subregion, unfavourable hydrogeological circumstances can be such that serious stresses like groundwater related droughts, subsidence or upconing of saline groundwater under abstraction wells can still occur.

4.1.1 Comparison to other studies

As shown in the introduction, there are several other studies carried out worldwide that make an estimation of the groundwater balance in perspective of groundwater volumes. As mentioned, MacDonald et al. (2012) compared the groundwater resources of Africa to the possibility to sustainably abstract groundwater. They showed that the aquifer productivity (the yield that can be expected from a borehole), is only high in northern Africa. This is because the groundwater volumes in these regions are sufficiently large to sustain interannual recharge variability. In this study, the same conclusion is drawn; sustainable and robust abstractions can only occur in regions where the groundwater volumes are large enough, even if the long-term average recharge is high.



Gleeson et al. (2016) showed that it is important to distinguish the groundwater by age, and that only a small fraction of the total global groundwater volume can be considered to be modern groundwater (less than 50 years old). They argued that only the modern groundwater volume can be considered to be a renewable resource. Therefore, the estimations of the sustainability of the groundwater abstractions of this study can be further improved by incorporating the age of the groundwater. Within regions of deep groundwater volumes, this might mean that still a large part of the groundwater abstraction will be from non-renewable groundwater since the abstracted groundwater might be old (> 50 years) and replenishing the water will take a long time.

Another interesting case is the relatively wet Mekong delta where the economy boomed during these last 30 years. Most fresh groundwater in the Mekong Delta was recharged 60.000 – 12.000 years ago when sea-level was much lower. Presently, groundwater is hardly being recharged due to low permeable Holocene clayey layer which restricts precipitation to infiltrate into the deeper groundwater system. However, since 1995, groundwater extractions have been increased yearly and because replenishment to the deeper groundwater system is very limited, groundwater level have dropped accordingly, leading to a severe land subsidence (Minderhoud et al., 2017; Pham et al., 2019). So even when fresh groundwater volumes are very large and abstractions are moderate for an area as big as the Mekong delta is, the impacts can be serious.

Thorweihe et al. (2002) also showed for the Nubian Aquifer System in North-East of Africa that although there are very large available groundwater volumes, the water is very old and the low groundwater recharge results in little replenishment. Furthermore, they stressed that groundwater abstractions will result in local drawdowns of the groundwater table. The abstractions are not sustainable in spite of the large volume in the aquifer.

4.1.2 Consequences of groundwater overexploitation

The previous section has shown that there are multiple areas in Europe that are threatened by groundwater overexploitation. There are several problems that may arise when the groundwater abstractions are large.

Salinization of the groundwater resources can be a result of extracting groundwater. Pumping of fresh groundwater results in upconing of the saline groundwater that is present below the fresh groundwater resources, which also results in the mixing of fresh and saline groundwater. Even when there are large bodies of fresh groundwater, it could still mean that groundwater wells become saline. Several studies have shown that for smaller fresh groundwater volumes, or for large abstraction fluxes, the salinization can more rapidly taking place (Bear and Dagan, 1964; Jakovovic et al., 2016).

Beside the sensitivity to salinization, pumping of groundwater can also induce subsidence, due to compaction of aquifers caused by a decrease in hydraulic head (Shirzaei et al., 2021; Nicholls et al., 2021). These rates can be very high, up to 30 cm per year in some areas, which exceeds the rates of global sea level rise (about 0.3 cm/year) (Ingebritsen and Galloway, 2014). A study of the Mekong Delta in Vietnam also calculated that the subsidence was about 1 cm/year due to groundwater abstractions, while the abstractions were still lower than the groundwater recharge on a yearly basis (Minderhoud et al., 2017). This is mainly caused by the geology of the area, where low-permeable clay layers at shallow depths inhibited the groundwater recharge to replenish the deeper aquifers.



Overexploitation of groundwater lead to lower groundwater levels (Custodio, 2002) and can also lower the (phreatic) water table, which poses a problem for crops and plants when the (phreatic) water table drops below the root zone. This can result in irreversible damage to nature areas and threatens the food security if crops cannot grow optimally (Van Loon, 2015; Malakoff et al., 2020).

Furthermore, there are other factors that threaten the water availability and increase the vulnerability to droughts. The first is climate change, which can have a big impact (Taylor et al., 2013; Green et al., 2011): it can result in a decrease in groundwater recharge and might increase the water demand. Secondly, sea level rise will have an impact on the water availability in coastal regions (e.g. Befus et al., 2020; Oude Essink et al., 2010). Sea level rise can lead to an increase of salt water intrusion and a decrease in the depth of the fresh-saline groundwater interface, which means that the groundwater volumes will decrease. However, the exploitation of groundwater in coastal regions has the most impact on the vulnerability of the coastal aquifers, the effect of sea level rise is smaller (Ferguson and Gleeson, 2012; Ketabchi et al., 2016). Thirdly, socio-economic changes may result in a higher water demand, and consequently a larger groundwater abstraction. Also, urbanization results in an increase in surface sealing which inhibits precipitation to infiltrate into the groundwater reservoirs.

4.2 Turnover time

The turnover time of the groundwater can be estimated by dividing the total groundwater volume by the groundwater recharge, assuming that a groundwater system can be approximated by linearly mixed reservoir (van Ommen, 1985; Raats, 1981; Van der Molen et al., 1989; Broers, 2004). In such a system the characteristic time, or turnover time T , is obtained by a simple volume divided by recharge flux approach. The turnover time is then mean travel time in the system and the travel time distribution follows an exponential curve. In such a system 95% of the flux has been drained to after 3 times the characteristic time, so after $3 \times T$. Raats (1981) showed that the turnover time can then be approximated 2D by $T = (\text{porosity} \times \text{thickness of the active aquifer system})$ divided by the recharge flux.

Calculating the turnover time by dividing the volume of the groundwater system by the recharge to the system thus gives an indication of the average time that groundwater will reside in the aquifer before it gets drained into the river system. This is a crude estimation: in reality it is possible that the shallow groundwater gets replenished fast, while replenishing the groundwater in the deeper aquifers might take a very long time. Whether the complete groundwater system is involved in the fresh groundwater flow, or that only the upper part is active, is not easily determined at European scale. It would require that we know the complete aquifer/aquitard structure and have a good estimate of the vertical hydraulic conductivities over that profile. We found that the hydraulic conductivities that were collected in GeoERA RESOURCE were not enough harmonized in the current setup, and the groundwater systems not characterized enough to allow more detail in the calculation of turnover times. Therefore, we limited ourselves to a calculation for the complete groundwater volume (Figure 3.10 or Figure 4.3, left) and a calculation for an estimate of the volume in the upper 100 m of the subsurface. For the “upper 100 m” calculation, we assumed that aquitards below 100 m depth would limit the flux to deeper layers and we neglected the part of the turnover time of the deeper part of the active flow system.

The turnover time (groundwater volume / groundwater recharge) is shown in Figure 4.3 (which is a copy of Figure 3.10) with the left figure showing the estimated turnover time based on the total groundwater volume and the right figure for the groundwater volume of the upper 100 m.

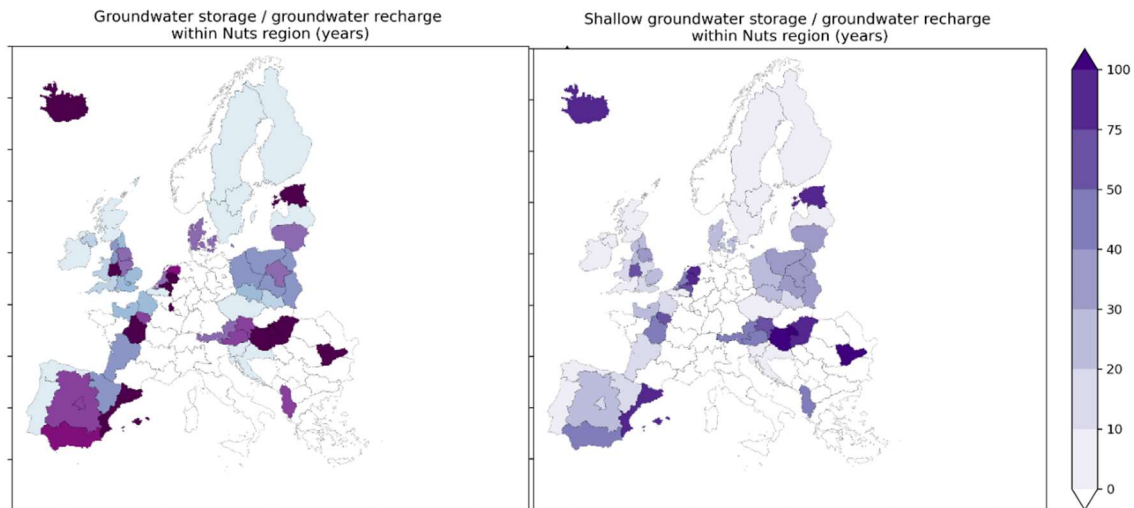


Figure 4.3 This is a copy of Figure 3.10. The total groundwater volume (km^3) divided by the groundwater recharge (km^3/year), which shows the turnover time of the groundwater. Left: turnover time based on the complete available groundwater volume. Right: turnover time for the volume in the upper 100 m of the subsurface.

Regions with thin aquifers and limited effective porosity (small groundwater volume) or wet regions (high groundwater recharge) have the shortest turnover times (light colors). The wet regions are generally found in the northern parts of Europe, like Scandinavia and Scotland. In Portugal, Croatia and Slovenia the groundwater volumes are small which result in shorter turnover times. The regions in Spain show a large difference between the maps which incorporate the full groundwater volume or the shallow groundwater volume. This is due to the occurrence of very deep groundwater volumes, whereas the groundwater volume in the upper 100 m is more limited.

It needs to be stressed that the maps of Figure 3.10 / Figure 4.1 represent only the saturated flow. Lag times in the unsaturated zone, which may be considerable, are not included and should be considered as well (see GeoERA HOVER Deliverable 5.3 (Ascott et al., 2020) for more details).

The turnover times also indicate the average residence time for pollutants in the groundwater. Areas with limited turnover times typically see higher average concentrations of contaminants over the saturated depth of the groundwater system and a faster response of the connected river water system. This means: faster increase of concentrations of groundwater seeping into the stream after the pollution starts, but also faster decrease after a pollution has stopped (Broers and Van Geer 2005, Kaandorp et al. 2021). Contrary, a system with long turnover times will only have high pollutant concentrations in the upper part of the groundwater system and the outflow to river systems will be strongly diluted by the outflow of older, non-polluted groundwater. However, the pollution of the receiving water may last longer, although at lower concentrations over the whole pollution history.



The third combined maps in Figure 3.10 / Figure 4.3 indicate that longer turnover times are present in the main sedimentary basins of Europe, including the Pannonian Basin in Hungary and surrounding countries, the Romanian Danube basin, the Paris basin, the Aquitaine basin, the Spanish basins around Valencia and Catalonia and the lower Rhine basins from the Netherlands and adjacent Germany. Except for the Spanish basins which do not receive large amounts of groundwater recharge, all of these basins have a relatively large buffer capacity to periods of drought or intensive pumping. The Spanish basins are more vulnerable for large scale groundwater abstractions, but the turnover maps indicate that a paleo groundwater resource may provide a lower vulnerability for contamination of the whole groundwater system.



5 CONCLUSIONS AND RECOMMENDATIONS

This study presented a first estimation of the water balance of EU's principal groundwater resources. This gives a first insight in the long-term sustainability and the robustness of groundwater abstractions. The study showed that three aspects will influence the vulnerability of the groundwater resources in a region.

- First, a large total groundwater volume will result in a more robust system that can absorb fluctuations due to rapid, incidental events, like prolonged droughts, or some decennia of overexploitation.
- Second, a large groundwater recharge results in a system that is resilient to stresses like abstraction.
- Third, less groundwater abstraction causes less stress on the system.

The study output shows that the regions in the Mediterranean and the densely populated areas are at the limits of the renewable groundwater that can be abstracted, because the abstracted groundwater volume is close to the volume of long-term average groundwater recharge. Furthermore, some regions are even more vulnerable since the available fresh groundwater volumes are limited which limits the buffer capacity in relation to periods of droughts and/or higher water demands. The regions where the fraction of the available groundwater volume over the groundwater abstraction is small (like Spain or the Czech Republic), the system appear to be less robust to withstand variations in annual recharge. Lastly, the combination of groundwater volumes over groundwater recharge gives insight in the turnover time of the groundwater. Relatively wet regions (Scandinavia or Scotland) or regions with thin aquifers (Portugal or Slovenia) have small turnover times. Longer turnover times mean that contaminants will reside in the groundwater for a longer period but discharge to the river system will show lower concentration of pollutants.

There are several recommendations to further elaborate and improve these results.

- To improve the estimation of the available groundwater resources, the occurrence of semi-permeable layers (aquitards) should also be incorporated. Within this study, the groundwater recharge is regarded as the water source that can replenish the full groundwater volume. In reality, even with high groundwater recharges, deeper groundwater resources can still become depleted. This can be due to the occurrence of low permeable layers, like clay layers, which prevent water from percolating from the upper groundwater to deeper groundwater (Neuzil, 1986). Therefore, the groundwater recharge will not reach the deeper aquifers and these groundwater resources might still be under stress.
- In line with the previous point, the depth of the groundwater abstractions should be studied to better estimate the effect of the abstractions on the groundwater resources. If the groundwater abstractions are at greater depths, they might deplete the groundwater resources that are hardly replenished by the groundwater recharge, since the recharge can hardly reach the deeper aquifers.
- To be able to derive the influence of low-permeable layers, there should be a unified approach to derive the horizontal and vertical hydraulic conductivities. For this study, the approach that was used by individual countries varied strongly, which resulted in widely different estimations for hydraulic conductivities of low-permeable layers (Neuzil, 1994).
- The differences between the newly developed pan-European groundwater recharge map and the groundwater recharge as calculated by the PCR-GLOBWB model indicate that the modelled groundwater recharge might be uncertain, while it is an important



quantity to determine the sustainability of groundwater resources. For future estimations, it might be good to improve the recharge (e.g. using the TACTIC map of Martinsen et al., 2021).

- The turnover time of groundwater in the unsaturated zone should be incorporated to better estimate the total turnover time of the groundwater. Within the GeoERA project 'HOVER', an estimation is made of the residence time in the unsaturated zone for a number of participating countries (Ascott et al., 2020), which in some regions exceeds 10 years (see Figure 5.1). Incorporating these times with the turnover times that are estimated in this study, will improve the estimation of the residence time of pollutants in the groundwater.
- The relation between groundwater volume, recharge and abstraction can further be quantified and should be combined with geology. For this, conceptual models should be improved, and site-specific, regional or even continental fully 3D numerical deterministic models of groundwater flow and groundwater quality transport should be used; the latter option is possibly available within a few years (e.g. De Graaf, et al., 2019; Verkaik et al., 2021a, 2021b).

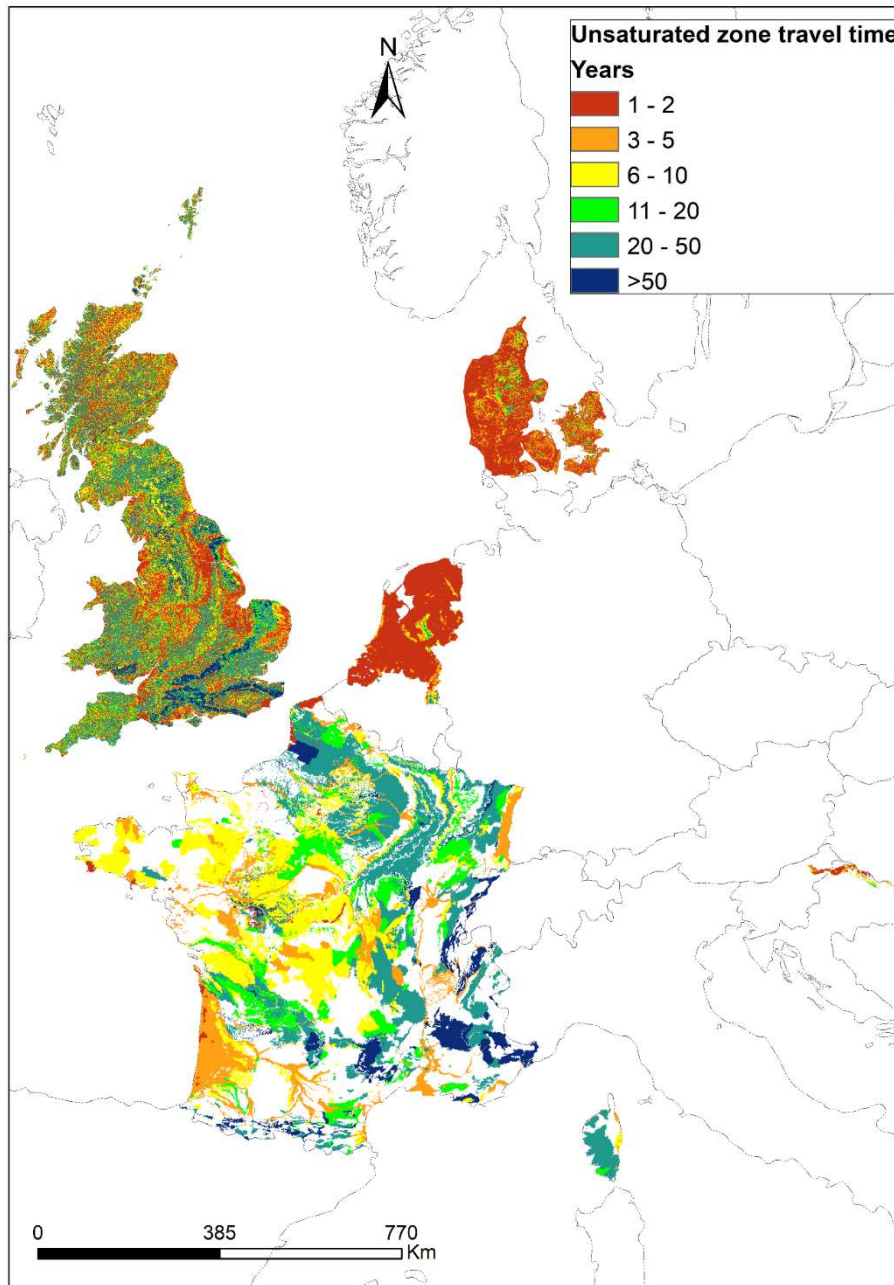


Figure 5.1 Travel times for nitrate in the unsaturated zone across selected pilots in this deliverable (after Ascott et al. 2021).



6 REFERENCES

- Ascott, M., Wang, L., Broers, H.P., van Vliet, M., Janssen, G., Gourcy, L., Pinson, S., Malcuit, E., Surdyk, N., Larva, O., Brkić, Z., Debattista, H., Rosenbom, A., Hinsby, K., Urbanc, J., Tedd, K., 2020. Deliverable 5.3. Modelling nitrate and pesticide transport: Assessments of N travel times. GeoERA HOVER.
- Broers, H.P. 2004. The spatial distribution of groundwater age for different geohydrological situations in the Netherlands: implications for groundwater quality monitoring at the regional scale. *Journal of Hydrology*, 299(1-2), 84-106.
- Broers, H.P. & Van Geer, F.C. 2005. Monitoring strategies at phreatic wellfields: A 3D travel time approach. *Groundwater*, 43(6), 850-862.
- Bear, J., Dagan, G., 1964. Some exact solutions of interface problems by means of the hodograph method. *J. Geophys. Res.* 69, 1563-1572. <https://doi.org/10.1029/JZ069i008p01563>
- Befus, K.M., Barnard, P.L., Hoover, D.J., Finzi Hart, J.A., Voss, C.I., 2020. Increasing threat of coastal groundwater hazards from sea-level rise in California. *Nat. Clim. Chang.* 10. <https://doi.org/10.1038/s41558-020-0874-1>
- Copernicus Climate Change Service (2017): ERA5: Fifth generation of ECMWF atmospheric reanalyses of the global climate. Climate Data Store (CDS) of the Copernicus Climate Change Service (C3S). <https://cds.climate.copernicus.eu/cdsapp#!/home>
- Custodio, E., 2002. Aquifer overexploitation: what does it mean? *Hydrogeology Journal* 10, 254–277. <https://doi.org/10.1007/s10040-002-0188-6>
- Custodio, E., Bruggeman, G.A., 1987. *Groundwater Problems in Coastal Areas, Studies and Reports in Hydrology (UNESCO)*. UNESCO, International Hydrological Programme, Paris.
- De Graaf, I.E.M., Gleeson, T., Van Beek, L.P.H., Sutanudjaja, E.H., Bierkens, M.F.P., 2019. Environmental flow limits to global groundwater pumping. *Nature* 574. <https://doi.org/10.1038/s41586-019-1594-4>
- Döll, P., Fiedler, K., 2008. Global-scale modeling of groundwater recharge. *Hydrol. Earth Syst. Sci. Discuss.* 12, 4069–4124. <https://doi.org/10.5194/hess-12-863-2008>
- Erban, L.E., Gorelick, S.M., Zebker, H.A., 2014. Groundwater extraction, land subsidence, and sea-level rise in the Mekong Delta, Vietnam. *Environ. Res. Lett.* 9, 084010. <https://doi.org/10.1088/1748-9326/9/8/084010>
- Ferguson, G., Gleeson, T., 2012. Vulnerability of coastal aquifers to groundwater use and climate change. *Nat. Clim. Chang.* 2, 342-345. <https://doi.org/10.1038/nclimate1930>
- Gleeson, T., Befus, K.M., Jasechko, S., Luijendijk, E., Cardenas, M.B., Bayani Cardenas, M., 2016. The global volume and distribution of modern groundwater. *Nat. Geosci.* 9, 161–164. <https://doi.org/10.1038/ngeo2590>
- Green, T.R., Taniguchi, M., Kooi, H., Gurdak, J.J., Allen, D.M., Hiscock, K.M., Treidel, H., Aureli, A., 2011. Beneath the surface of global change: Impacts of climate change on groundwater. *J. Hydrol.* 405, 532–560. <https://doi.org/10.1016/j.jhydrol.2011.05.002>
- Gunnink, J.L., Pham, V.H., Oude Essink, G.H.P., Bierkens, M.F.P., 2021. The 3D groundwater salinity distribution and fresh groundwater volumes in the Mekong Delta, Vietnam, inferred from geostatistical analyses. *Earth Syst. Sci. Data* 13, 3297–3319. <https://doi.org/10.5194/essd-13-3297-2021>
- Haitjema, H.M., 1995. On the residence time distribution in idealized groundwatersheds, *Journal of Hydrology*, 172, 127-146.
- Ingebritsen, S.E., Galloway, D.L., 2014. Coastal subsidence and relative sea level rise. *Environ. Res. Lett.* 9, 091002. <https://doi.org/10.1088/1748-9326/9/9/091002>



- Jakovovic, D., Werner, A.D., De Louw, P.G.B., Post, V.E.A., Morgan, L.K., 2016. Saltwater upconing zone of influence. *Adv. Water Resour.* 94, 75-86. <https://doi.org/10.1016/j.advwatres.2016.05.003>
- Kaandorp, V.P., Broers, H.P., Van Der Velde, Y., Rozemeijer, J. & De Louw, P.G.B. 2021. Time lags of nitrate, chloride, and tritium in streams assessed by dynamic groundwater flow tracking in a lowland landscape. *Hydrology and Earth System Sciences*, 25(6), 3691-3711.
- Ketabchi, H., Mahmoodzadeh, D., Ataie-Ashtiani, B., Simmons, C.T., 2016. Sea-level rise impacts on seawater intrusion in coastal aquifers: Review and integration. *J. Hydrol.* 535. <https://doi.org/10.1016/j.jhydrol.2016.01.083>.
- Kivits, T., Broers, H.P., Janza, M., 2020. Deliverable 6.2. Database with information on volumes and depths at 10x10 and/or 25x25 km grids. GeoERA RESOURCE.
- Kivits, T., Broers, H.P., Berendrecht, W., 2021. Deliverable 6.3. Maps showing the depth and volume of fresh groundwater. GeoERA RESOURCE.
- MacDonald, A.M., Bonsor, H.C., Dochartaigh, B.É.Ó., Taylor, R.G., Knox, J., Hess, T., Daccache, A., Ferguson, I.M., Maxwell, R.M., Döll, P., 2012. Quantitative maps of groundwater resources in Africa. *Environ. Res. Lett.* 7, 024009. <https://doi.org/10.1088/1748-9326/7/2/024009>
- Malakoff, D., Sugden, A., Ash, C., Hines, P., Rai, T., Smith, J., 2020. Drought; Special Section. *Science*.
- Martinsen, G., H. Bessiere, Y. Caballero, J. Koch, A. J. Collados-Lara, M. Mansour, O. Sallasmaa, D. Pulido Velázquez, T. Hunter Williams, W.J. Zaadnoordijk and S. Stisen (2021) Pan-European high-resolution groundwater recharge mapping – combining satellite data and national survey data using machine learning. Submitted.
- Micallef, A., Person, M., Berndt, C., Bertoni, C., Cohen, D., Dugan, B., Evans, R., Haroon, A., Hensen, C., Jegen, M., Key, K., Kooi, H., Liebetrau, V., Lofi, J., Mailloux, B.J., Martin-Nagle, R., Michael, H.A., Müller, T., Schmidt, M., Schwalenberg, K., Trembath-Reichert, E., Weymer, B., Zhang, Y., Thomas, A.T., 2021. Offshore Freshened Groundwater in Continental Margins. *Rev. Geophys.* 59, 1–54. <https://doi.org/10.1029/2020rg000706>
- Minderhoud, P.S.J., Erkens, G., Pham, V.H., Bui, V.T., Erban, L.E., Kooi, H., Stouthamer, E., 2017. Impacts of 25 years of groundwater extraction on subsidence in the Mekong delta, Vietnam. *Environ. Res. Lett.* 12, 13. <https://doi.org/10.1088/1748-9326/aa7146>
- Neussner, O., 2019. Trouble underground – Land Subsidence in the Mekong Delta.
- Neuzil, C.E., 1986. Groundwater flow in low-permeability environments. *Water Resour. Res.* 22, 1163–1195. <https://doi.org/10.1029/WR022i008p01163>
- Neuzil, C.E., 1994. How permeable are clays and shales? *Water Resour.* 30, 145–150.
- Nicholls, R.J., Lincke, D., Hinkel, J., Brown, S., Vafeidis, A.T., Meyssignac, B., Hanson, S.E., Merkens, J., Fang, J., 2021. A global analysis of subsidence, relative sea-level change and coastal flood exposure. *Nat. Clim. Chang.* 45. <https://doi.org/10.1038/s41558-021-00993-z>
- Oude Essink, G.H.P., Van Baaren, E.S., De Louw, P.G.B., 2010. Effects of climate change on coastal groundwater systems: A modeling study in the Netherlands. *Water Resour. Res.* 46, 1–16. <https://doi.org/10.1029/2009WR008719>
- Pham, V.H., Van Geer, F.C., Bui, V.T., Dubelaar, W., Oude Essink, G.H.P., 2019. Paleo-hydrogeological reconstruction of the fresh-saline groundwater distribution in the Vietnamese Mekong Delta since the late Pleistocene. *J. Hydrol. Reg. Stud.* <https://doi.org/10.1016/j.ejrh.2019.100594>
- Post, V.E.A., Groen, J., Kooi, H., Person, M., Ge, S., Edmunds, W.M., 2013. Offshore fresh groundwater reserves as a global phenomenon. *Nature* 504, 71–8. <https://doi.org/10.1038/nature12858>
- Raats, P.A.C. 1981. Residence times of water and solutes within and below the root zone. *Agricultural Water Management*, 4(1-3), 63-82.



- Shirzaei, M., Freymueller, J., Törnqvist, T.E., Galloway, D.L., Dura, T., Minderhoud, P.S.J., 2020. Measuring, modelling and projecting coastal land subsidence. *Nat. Rev. Earth Environ.* <https://doi.org/10.1038/s43017-020-00115-x>
- Sutanudjaja, E. H., van Beek, R., Wanders, N., Wada, Y., Bosmans, J. H. C., Drost, N., van der Ent, R. J., de Graaf, I. E. M., Hoch, J. M., de Jong, K., Karssenber, D., López López, P., Peßenteiner, S., Schmitz, O., Straatsma, M. W., Vannamettee, E., Wisser, D., and Bierkens, M. F. P.: PCR-GLOBWB 2: a 5 arcmin global hydrological and water resources model, *Geosci. Model Dev.*, 11, 2429-2453, <https://doi.org/10.5194/gmd-11-2429-2018>, 2018.
- Stuurman, R.J., Baggelaar, P., Berendrecht, W.L., Buma, J.T., De Louw, P.G.B., Oude Essink, G.H.P., 2008. *In Dutch: Toekomst van de Nederlandse grondwatervoorraad in relatie tot klimaatverandering*, TNO-rapport 2008-U-R0074/B.
- Stuyfzand, P.J., 1993. Hydrochemistry and hydrology of the coastal dune area of the Western Netherlands. Vrije Universiteit, Amsterdam. <https://doi.org/10.1017/CBO9781107415324.004>
- Taylor, R.G., Green, T.R., Scanlon, B.R., Döll, P., Rodell, M., Van Beek, L.P.H., Wada, Y., Longuevergne, L., Leblanc, M., Famiglietti, J.S., Edmunds, M., Konikow, L.F., Green, T.R., Chen, J., Taniguchi, M., Bierkens, M.F.P., MacDonald, A.M., Fan, Y., Maxwell, R.M., Yechieli, Y.Y., Gurdak, J.J., Allen, D.M., Shamsudduha, M., Hiscock, K.M., Yeh, P.J.F., Holman, I., Treidel, H., 2013. Ground water and climate change. *Nat. Clim. Chang.* 3, 1–8. <https://doi.org/doi:10.1038/nclimate1744>
- Thorweihe, U., Heintz, M., 2002. Groundwater resources of the Nubian Aquifer System: NE-Africa. *Aquifers major basins—non-renewable water Resour. Modif. Synth.*
- Van Loon, A.F., 2015. Hydrological drought explained. *Wiley Interdiscip. Rev. Water* 2, 359–392. <https://doi.org/10.1002/wat2.1085>
- Van Ommen, H.C. 1985. The “mixing-cell” concept applied to transport of non-reactive and reactive components in soils and groundwater. *Journal of Hydrology*, 78(3-4), 201-213.
- Van Ommen, H.C., Van Genuchten, M.T., Van der Molen, W.H., Dijk, R. & Hulshof, J. 1989. Experimental and theoretical analysis of solute transport from a diffuse source of pollution. *Journal of Hydrology*, 105(3-4), 225-251.
- Verkaik, J., Sutanudjaja, E.H., Oude Essink, G.H.P., Lin, H.X., Bierkens, M.F.P., 2021a. Implementing a transient PCR-GLOBWB-MODFLOW global groundwater model on a 1 km resolution using high performance computing, in: AGU Fall Meeting 2021.
- Verkaik, J., Van Engelen, J., Huizer, S., Bierkens, M.F.P., Lin, H.X., Oude Essink, G.H.P., 2021b. Distributed memory parallel computing of three-dimensional variable-density groundwater flow and salt transport. *Adv. Water Resour.* 154, 103976. <https://doi.org/10.1016/j.advwatres.2021.103976>
- Werner, M., Schellekens, J., Gijsbers, P., Van Dijk, M.J., Van den Akker, O., Heynert, K., 2013. The Delft-FEWS flow forecasting system. *Environ. Model. Softw.* 40, 65–77. <https://doi.org/10.1016/j.envsoft.2012.07.010>.
- Witte, J.-P.M., De Louw, P.G.B., Van Ek, R., Bartholomeus, R., Van den Eertwegh, G., Gilissen, H.K., Van Rijswijk, M., Beugeling, G., Ruijtenberg, R., Van der Kooij, W., 2020. Aankomst droogte vraagt transitie waterbeheer (in English: Tackling drought asks for a transition in water management). *Water Governance.* 120–131.
- Zamrsky, D., 2021. Current and future state of groundwater in coastal unconsolidated sediment systems worldwide, PhD thesis Utrecht University, The Netherlands.